Available online at www.sciencedirect.com
SCIENCE DIRECT®
Geochimica et Cosmochimica Acta 70 (2006) 1904–1913
Geochimica
www.elsevier.com/locate/gca

Pressure effects on the reduced partition function ratio for hydrogen isotopes in water

V.B. Polyakov [a,*], J. Horita [b], D.R. Cole [b]

[a] Institute of Experimental Mineralogy, Russian Academy of Science, Chernogolovka, Moscow Region, Russia
[b] Chemical Sciences Division, Oak Ridge National Laboratory, Oak Ridge, TN 37831-6110, USA

Received 15 June 2005; accepted in revised form 18 January 2006

Abstract

We have developed a simple, yet accurate theoretical method for calculating the reduced isotope partition function ratio (RIPFR) for hydrogen of water at elevated pressures. This approach requires only accurate equations of state (EOS) for pure isotopic end-members (H_2O and D_2O), which are available in the literature. The effect of pressure or density on the RIPFR of water was calculated relative to that of ideal-gas water at infinitely low pressure for the temperature range from 0 to 527 °C. For gaseous and low-pressure (ca. $\leqslant$15 MPa) supercritical phases of water, the RIPFR increases slightly (1–1.3‰) with pressure or density in a fashion similar to those of many other geologic materials. However, in liquid and high-pressure (>20 MPa) supercritical phases, the RIPFR of water decreases (0.5–6‰) with increasing pressure (or density) to 100 MPa. This rather unique phenomenon is ascribed to the inverse molar volume isotope effects (MVIE) of liquid and high-density supercritical waters, $V(D_2O) > V(H_2O)$, while other substances including minerals show the normal MVIE. These theoretical predictions were experimentally confirmed by Horita et al. [Horita, J., Cole, D.R., Polyakov, V.B., Driesner, T., 2002. Experimental and theoretical study of pressure effects on hydrogen isotope fractionation in the system brucite–water at elevated temperatures. *Geochim. Cosmochim. Acta* **66**, 3769 – 3788.] for the system brucite–water. Although the P–T ranges for the EOS of normal and heavy waters are rather limited, our modeling indicates that the RIPFR of water continues to decrease with pressure above 100 MPa. The method developed here can be applied to any other geologic fluids, if accurate EOS for their isotopic end-members is available. These results have important implications for the interpretation of high-pressure isotopic partitioning in the Earth, the outer planets, and their moons.

1. Introduction

A quantitative understanding of the isotopic properties of water and other fluids are of great importance to the interpretation of isotopic behavior not only at elevated temperatures, but also at elevated pressures. Trace amounts of water have been reported for various nominally anhydrous minerals from the mantle (Williams and Hemley, 2001), suggesting that water may be more abundant in the deep Earth than previously thought, especially in subduction zones. The outer planets and their moons in the solar system also contain water (ice), methane, and other fluids at elevated pressures. Despite the primary importance of pressure as a master variable in controlling phase equilibria and elemental distributions, our understanding is limited on how pressure affects the isotopic properties of fluids. Since the pioneering works by Singh and Wolfsberg (1975) and Bigeleisen and Mayer (1947) in the 1940s, many investigators reported their results of statistical–mechanical calculations of the reduced isotopic partition function ratios (RIPFR) of water and other simple molecules, which provide information on isolated molecules, i.e., ideal-gas at infinitely low pressures. Calculations by Wolfsberg and co-workers (Bron et al., 1973; Kleinman and Wolfsberg, 1973; Bardo and Wolfsberg, 1975, 1977) and by Richet et al. (1977) are among the most

* Corresponding author. Fax: +495 938 2054.
E-mail address: polyakov@iem.ac.ru (V.B. Polyakov).

0016-7037/$ - see front matter © 2006 Elsevier Inc. All rights reserved.
doi:10.1016/j.gca.2006.01.010

accurate and updated calculations, including anharmonic, rotational and rotational-vibration corrections.[1] Although small errors and uncertainties exist regarding the anharmonic corrections, the RIPFR of "ideal-gas" water is well determined.

The calculation of the RIPFR for liquids and supercritical fluids at elevated pressures by means of the statistical–mechanical methods requires accurate knowledge of both inter- and intra-molecular force fields and their contributions to the RIPFR over a wide range of temperature and pressure. Such detailed information on the structure and properties of fluids is currently not available even for water, the most studied fluid. To circumvent this problem, several approaches were used in the literature to construct simple models for the structure and properties of high-density fluids. For example, several investigators used an average molecular-cell model to calculate the RIPFR of liquid water (see a review by Jancso and Van Hook, 1974). Recently, Driesner (1997) estimated the pressure effect on RIPFR of supercritical water, assuming that only the internal symmetric O–H stretching frequency of water molecules red-shits with increasing pressure based on experimental IR data from the literature. However, these simplistic models and assumptions yield qualitative results at best.

Other methods utilized molecular-based simulations, which are becoming increasingly more powerful for isotopic studies. Bopp et al. (1974) and Driesner et al. (2000) calculated oxygen and hydrogen isotopic fractionation in the hydration complexes of dissolved electrolytes in water, using quantum-mechanical (Hartree–Fock and Density Function Theory, DFT) simulations. Driesner and Seward (2000) used classical mechanical (molecular dynamics, MD) and quantum mechanical (DFT) simulations to calculate oxygen and hydrogen isotope fractionations among different water clusters (monomer, dimmer, trimer, etc.) in the gas phase. Classical mechanics-based molecular simulations alone cannot be used to directly calculate isotopic effects, which have their origins in quantum mechanics. However, using the first- and second-order Kirkwood–Wigner quantum correction (perturbation method), Chialvo and Horita (2003) recently conducted MD and Gibbs Ensemble Monte Carlo simulations for the liquid–vapor and solid-vapor isotope fractionation of nobles gases (Ne, Ar, and Kr), including the compositional dependence of liquid–vapor fractionation of Ar and Kr isotopes. Their simulation results agree very well with experimental data in the literature.

In this study, we have developed a novel approach for calculating the RIPFR of fluids at elevated pressures, using thermodynamic data of isotopically pure end-members. All thermophysical properties (pressure–volume–temperature relationship, specific heat, entropy, etc.) of fluids are accurately described by equation of states (EOS). However, thermodynamic functions from the EOS cannot be applied directly to chemical reactions, especially to isotope fractionation. This is because free energies of isotopologues defined by the EOS's are not mutually consistent since the enthalpies of formation are not included in the values of isotopologues thermodynamic functions. The EOS approach, however, can provide accurate differences in the values of thermodynamic functions (free energy, chemical potential, enthalpy) of a given isotopic species between different pressure–volume–temperature (P–V–T) conditions. This, in turn, can provide a means of calculating differences in the reduced partition function of isotopic species relative to a reference P–T condition. Here, we present the principles of our new method for calculating the RIPFR of fluids on the basis of their EOS. We applied this method to water, the most important geologic fluid, to understand the effect of pressure on the RIPFR.

2. Equations of states for normal and heavy waters

Because of their primary importance in various disciplines of science and engineering, a number of equations of state (EOS) have been developed for both light (H_2O) and heavy water (D_2O) over a wide range of temperature and pressure in the literature. However, only a few of them (Hill et al., 1982; Kestin et al., 1984a,b) provide enough accuracy to calculate their isotopic properties for the both end-member fluids. Recently, several investigators (Kiselev, 1997; Kostrowicka-Wyczalkowska et al., 2000; Abdulkadirova et al., 2002) presented new crossover EOS for H_2O, D_2O, and their mixtures in the narrow P–T range near the critical point. Hill (1990) and Wagner and Pruss (2002) reported EOS for H_2O only. In the present study, we use the EOS developed by Kestin et al. (1984a,b) for H_2O and D_2O because of their high quality and internal consistency over a wide range of P–T conditions.

According to the formulation given by Kestin et al. (1984a,b), all equilibrium thermodynamic properties, exclusive of the region near the critical point, are represented by the canonical equation $A = A(T, \rho)$, where A is the Helmholtz free energy, T is absolute temperature (K), and ρ is the molar density (moles per unit volume). EOS

[1] The RIPFR is the main concept of stable isotope fractionation theory (Bigeleisen and Mayer, 1947; Urey, 1947). The RIPFR is defined as (Urey, 1947; Bigeleisen and Mayer, 1947; Singh and Wolfsberg, 1975):

$$(s^*/s)f = \frac{Q^*}{Q} \Big/ \left(\frac{Q^*}{Q}\right)_{\text{class}}$$

or in logarithmic form: $\ln(s^*/s)f = -\frac{A^*-A}{kT} + \left(\frac{A^*-A}{kT}\right)_{\text{class}}$,
where $\ln(s^*/s)f$ is the RIPFR, Q is the partition function (statistical sum), A is the Helmholtz free energy, k is the Boltzmann constant, T is absolute temperature, the asterisk $*$ refers to the isotopically substituted molecule, and the subscript "class" denotes quantities calculated according to classical (non-quantum) mechanics.

Equilibrium isotope fractionation factor between two substances A and B (α_{A-B}) can be expressed as:

$$\alpha_{A-B} = \frac{(s^*/s)f_A}{(s^*/s)f_B}.$$

for both D_2O and H_2O are written in a non-dimensional form and include numerous empirical coefficients. An appropriate formula for calculating the Helmholtz free energy is given by Kestin et al. (1984a,b). The temperature–pressure ranges of the EOS are:

H_2O:

$$P \leqslant 100[5 + (T - 273.15)/15] \text{ (MPa)}$$
$$\text{at } 273.15 \leqslant T \leqslant 423.15 \text{ (K)}$$

and

$$P \leqslant 1500 \text{ (MPa) at } 423.15 \leqslant T \leqslant 1273.15 \text{ (K)}$$

exclusive of the region around the critical point;

$$|T - T_{cr}| < 1K, |\rho/\rho_{cr} - 1| < 0.3,$$

where the subscript cr stands for the critical point.

D_2O:

$$P \leqslant 100 \text{ (MPa)}, T_{tr} \leqslant T \leqslant 800 \text{ (K)}$$

exclusive of the near-critical range:

$$0.991 \leqslant T/T_{cr} \leqslant 1.06 \text{ and } 0.7 \leqslant \rho/\rho_{cr} \leqslant 1.3,$$

where the subscript tr stands for the triple point. Although Kestin et al. (1984a,b) presented formulations of the EOS for H_2O and D_2O that cover the critical region, those formulations do not have the canonical form. For this reason, the critical region of water is not considered in this study.

EOS cannot be applied directly to computing the RIPFR because the enthalpies of formation of both water species are not available. Of course, we can compare the thermodynamic functions relative to those at the different states on the basis of the EOS. Unlike their partition functions, vapor pressure isotope effects (VPIE) of D_2O and H_2O (VPIE $= P_{H_2O}/P_{D_2O}$) can be directly evaluated from the EOS. This is not surprising because VPIE, which is the ratio of the saturation vapor pressures of two pure isotope species, can be calculated from the derivatives of their thermodynamic functions. Calculation of the VPIE from the EOS of H_2O and D_2O serves as a test for the accuracy of these EOS for calculating isotope effects. The saturation vapor pressure for light and heavy waters can be calculated using the condition that the chemical potentials of vapor and liquid phases are equal along the their boundary, equivalent to the zero value of Maxwell's integral between liquid and vapor phases.

$$\int_{\text{Liq}}^{\text{Vap}} \left(\frac{\partial G}{\partial P}\right)_T \mathrm{d}P = \int_{\text{Liq}}^{\text{Vap}} V \,\mathrm{d}P = 0, \quad (1)$$

where G is the Gibbs free energy and V is the molar volume. The integration is made along the entire isothermal line from the vapor (Vap) to the liquid (Liq) phase defined by the EOS (e.g., Kondepudi and Prigogine, 1998). Eq. (1) was solved numerically for the temperature range from 5 to 360 °C with 5 °C steps. Initial values at each temperature were estimated using the Clapeyron–Clausius equation, and results of the calculation for VPIE are given in Fig. 1. An agreement between experimental data and those calculated from the EOS is excellent. Differences between experimental and our calculated data do not exceed the experimental error of about 0.2%. Furthermore, the EOS yield a crossover temperature ($P_{H_2O}/P_{D_2O} = 1$) of 221.34 °C, which is in a good agreement with experimental data (221.00 °C by Zieborak, 1966 and 220.95 °C by Jancso and Van Hook, 1974). This agreement with experimental data attests to the accuracy of the EOS for calculating small differences in various isotopic properties between heavy and light water.

3. Principles of EOS-based methods for calculating the reduced isotope partition function ratio of real fluids

Here we present general principles for calculating the reduced partition function ratios using EOS of pure isotopic species. H_2O and D_2O serve as a good example, but the approaches presented below can be applied to any substance, if EOS is available for their pure isotopic species.

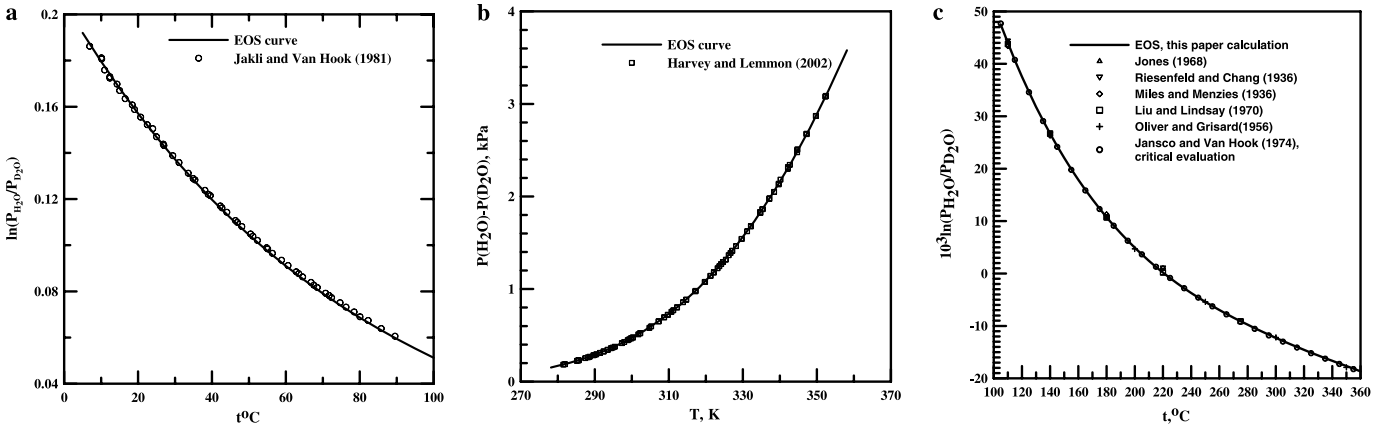

Fig. 1. Comparisons of VPIE calculated by the EOS with experimental data. (a) Comparison with data of Jàkli and Van Hook (1981) below 100 °C. (b) Comparison with data of Harvey and Lemmon (2002) below 100 °C. (c) Comparison with experimental data in the range from 100 to 360 °C. (See above-mentioned references for further informantion).

Two EOS-based methods are presented, which allow the calculation of the reduced partition function ratio of real H_2O–D_2O fluids relative to those of ideal-gas H_2O–D_2O. The latter has been reported in the literature by Wolfsberg and his co-workers (Bron et al., 1973; Kleinman and Wolfsberg, 1973; Bardo and Wolfsberg, 1975, 1977, 1978) and Richet et al. (1977).

3.1. Method 1

Bigeleisen (1961) presented a formula that relates the RIPFR of condensed phases to VPIE. Below, we reproduce his derivations with some modifications that are convenient for the use of the EOS. The Gibbs free energy for real-gas phase (G_r) can be written as

$$G_r/RT = \ln P - \frac{3}{2}\ln M - \frac{5}{2}\ln T + A_i/RT + Z + K_{ST}, \qquad (2)$$

where K_{ST} is the Sackur–Tetrode constant, M is the molecular weight, R is the gas constant, Z ($=PV/RT$) is the compressibility factor, and A_i is the Helmholtz free energy for molecular rotation and internal energy. The equilibrium condition between gaseous and condensed phases, $G_c = G_r$, where G_c is the Gibbs energies of condensed phase, for D_2O and H_2O leads to

$$\ln\left(\frac{P^*}{P}\right) = \frac{G_c^* - G_c}{RT} - \frac{A_i^* - A_i}{RT} + \frac{3}{2}\ln\left(\frac{M^*}{M}\right) - (Z^* - Z). \qquad (3)$$

Hereafter the asterisk denotes quantities relating to D_2O. Note the second and third terms of Eq. (3) represent the quantum-mechanical partition function for ideal-gas

$$-\frac{A_i^* - A_i}{RT} + \frac{3}{2}\ln\left(\frac{M^*}{M}\right) = \ln(Q^*/Q)_{quant} = \ln(s^*/s)f_{id} + \frac{3}{2}n\ln\frac{m^*}{m}, \qquad (4)$$

where Q is the ideal gas quantum partition function (statistical sum), $\ln(s*/s)f_{id}$ is the RIPFR of ideal-gas and m and $m*$ are the atomic masses of protium and deuterium, respectively. The n is the multiplicity of the isotope substitution (2 for D_2O). Unlike the Helmholtz free energy of ideal gas, the Gibbs free energy of condensed phases cannot be directly converted to the RIPFR, because the Gibbs energies in Eq. (3) refer to different pressures. Using the theorem of small increments (Landau and Lifshits, 1980), which claims $\delta G_{T,P} \approx \delta A_{T,V}$, and neglecting the second and higher-order terms

$$G(T,P^*,m^*) = G(T,P,m^*) + \int_P^{P^*}\left(\frac{\partial G}{\partial P}\right)_T dP = G(T,P,m^*) + \int_P^{P^*} V_c\, dP \cong G(T,P,m^*) + (P^* - P)V. \qquad (5)$$

Thus, the first term in the right-hand side of Eq. (3) can be written:

$$\frac{G_c(T,P^*,m^*) - G_c(T,P,m)}{RT} = \frac{G_c(T,P,m^*) - G_c(T,P,m)}{RT} + \frac{(P^* - P)V_c}{RT} = -\ln(s^*/s)f_c - \frac{3}{2}n\ln\frac{m^*}{m} + \frac{(P^* - P)V_c}{RT}. \qquad (6)$$

Inserting Eqs. (4) and (6) into Eq. (3), one obtains

$$\ln\left(\frac{P^*}{P}\right) = -[\ln(s^*/s)f_c - \ln(s^*/s)f_{id}] + \frac{(P^* - P)V}{RT} - (Z^* - Z). \qquad (7)$$

Using the relationship $\ln(P^*/P) \approx (P^* - P)/P$, Eq. (7) is rewritten

$$\ln\left(\frac{P^*}{P}\right)\left(1 - \frac{PV}{RT}\right) + (Z^* - Z) = -[\ln(s^*/s)f_c - \ln(s^*/s)f_{id}]. \qquad (8)$$

The temperature and pressure can be calculated from the EOS of H_2O and D_2O, at which Eq. (8) becomes zero

$$\ln(s^*/s)f_c(P_0,T_0) = \ln(s^*/s)f_{id}(T_0), \qquad (9)$$

where $T_0 = 244.76$ °C (517.91 K) and $P_0 = 3633.5438$ kPa (saturated vapor pressure of H_2O).

Using the definition of the RIPFR, Eq. (9), and $\ln(s^*/s)f_{id}(T_0) = 2.4122$ at $T_0 = 517.91$ K and $P_0 = 3633543.8$ Pa (Bron et al., 1973; Bardo and Wolfsberg, 1978), we obtain

$$\begin{aligned}
&\ln(s^*/s)f(P,T)\\
&= \frac{G(P,T) - G^*(P,T)}{RT} - \frac{3}{2}n\ln\frac{m^*}{m}\\
&= \frac{G(P,T) - G^*(P,T)}{RT} - \frac{G(P_0,T_0) - G^*(P_0,T_0)}{RT}\\
&\quad + \frac{G(P_0,T_0) - G^*(P_0,T_0)}{RT} - \frac{3}{2}n\ln\frac{m^*}{m}\\
&= \frac{G(P,T) - G(P_0,T_0)}{RT} - \frac{G^*(P,T) - G^*(P_0,T_0)}{RT}\\
&\quad + \frac{T_0}{T}\left[\frac{G(P_0,T_0) - G^*(P_0,T_0)}{RT_0} - \frac{3}{2}n\ln\frac{m^*}{m}\right] - \frac{3}{2}n\left(1 - \frac{T_0}{T}\right)\ln\frac{m^*}{m}\\
&= \frac{G(P,T) - G(P_0,T_0)}{RT} - \frac{G^*(P,T) - G^*(P_0,T_0)}{RT}\\
&\quad + \frac{T_0}{T}\ln(s^*/s)f_c(P_0,T_0) - \frac{3}{2}n\left(1 - \frac{T_0}{T}\right)\ln\frac{m^*}{m}\\
&= \frac{T_0}{T}\ln(s^*/s)f_{id}(T_0) + \frac{G(P,T) - G(P_0,T_0)}{RT}\\
&\quad - \frac{G^*(P,T) - G^*(P_0,T_0)}{RT} - \frac{3}{2}n\left(1 - \frac{T_0}{T}\right)\ln\frac{m^*}{m}\\
&= \frac{T_0}{T}2.4122 + \frac{G(P,T) - G(P_0,T_0)}{RT} - \frac{G^*(P,T) - G^*(P_0,T_0)}{RT}\\
&\quad - \frac{3}{2}n\left(1 - \frac{T_0}{T}\right)\ln\frac{m^*}{m} \quad (\text{at } T_0 = 517.91\ \text{K}).
\end{aligned} \qquad (10)$$

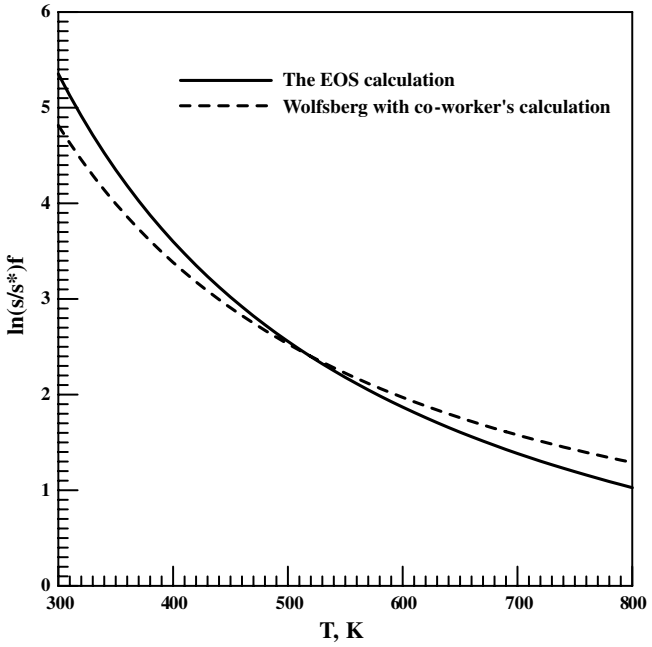

Fig. 2. Comparison of the 'ideal-gas' RIPFR for D_2O–H_2O calculated from the EOS (Method 1) with that by statistical–mechanical method (Bron et al., 1973; Bardo and Wolfsberg, 1975, 1977, 1978).

This equation allows one to calculate the RIPFR of real-fluids of H_2O–D_2O on the basis of their EOS. A reference point P_0–T_0 can be chosen arbitrarily along the vapor–liquid boundary, including those that yield non-zero value of Eq. (8). In such a case, a non-zero term has to be added to the right-hand side of Eq. (9).

The validity of Eq. (10) can be tested by comparing results of the RIPFR of ideal-gas H_2O–D_2O at the limit of low density with statistical–mechanical calculations by Richet et al. (1977), and Wolfsberg and co-workers (Bron et al., 1973; Kleinman and Wolfsberg, 1973; Bardo and Wolfsberg, 1975, 1977, 1978). A large discrepancy is observed in the temperature dependency between the ideal-gas RIPFR, which is calculated using the EOS, and those calculated by the statistical–mechanical approach (Fig. 2). This large discrepancy is most likely due to the fact that the ideal-gas part of EOS of D_2O (Kestin et al., 1984b) does not have the same accurate formalism as that for H_2O (Kestin et al., 1984a). This deficiency should be addressed in future developments of EOS for D_2O.

3.2. Method 2

At the low density limit ($\rho \to 0$), the EOS for pure fluids is reduced to that for the ideal-gas. Thus, if we can calculate pressure (and density) derivatives of thermodynamic properties of H_2O and D_2O from their ideal-gas counterparts using EOS, pressure (density) effects on their thermodynamic properties can be obtained, including the RIPFR:

$$\begin{aligned}
&\ln(s^*/s)f(T,\rho)\\
&=\frac{A(T,\rho)-A^*(T,\rho)}{RT}-\frac{3}{2}n\ln\frac{m^*}{m}=\frac{A(T,0)-A^*(T,0)}{RT}\\
&\quad-\frac{3}{2}n\ln\frac{m^*}{m}+\frac{A(T,\rho)-A^*(T,0)}{RT}-\frac{A^*(T,\rho)-A^*(T,0)}{RT}\\
&=\ln(s^*/s)f_{\mathrm{id}}(T)+\frac{A(T,\rho)-A(T,0)}{RT}-\frac{A^*(T,\rho)-A^*(T,0)}{RT},
\end{aligned} \tag{11}$$

where $A(T,0)=\lim_{\rho\to 0}A(T,\rho)$. It should be stressed that the molar density (molar volume) in Eq. (11) must be the same for H_2O and D_2O. An analogous expression of Eq. (11) can be written in terms of the Gibbs free energy and pressure, which is more convenient to compare with experimental data

$$\begin{aligned}
\ln(s^*/s)f(T,P)&=\ln(s^*/s)f_{\mathrm{id}}(T)+\frac{G(T,P)-G(T,0)}{RT}\\
&\quad-\frac{G^*(T,P)-G^*(T,0)}{RT},
\end{aligned} \tag{12}$$

where $G(T,0)\equiv\lim_{P\to 0}G(T,P)$. Thus, the deviation of the RIPFR of a real fluid is defined by pressure dependency of the Gibbs free energies of light and heavy isotopic molecules. This method requires the knowledge of the ideal-gas RIPFR over the entire temperature range of interest, instead of any single point of P–T used in the first method. Using the relationship, $V=(\partial G/\partial P)_T$, Eq. (12) can be rewritten as

$$\begin{aligned}
&\ln(s^*/s)f(T,P)-\ln(s^*/s)f_{\mathrm{id}}(T)\\
&=\int_0^P\frac{V}{RT}\,\mathrm{d}P-\int_0^P\frac{V^*}{RT}\,\mathrm{d}P=-\int_0^P\frac{V^*-V}{RT}\,\mathrm{d}P.
\end{aligned} \tag{13}$$

Thus, the success of this method depends entirely on the accuracy of thermodynamic data, particularly for the molar volume isotope effect (MVIE); $\Delta V=V^*-V$, of EOS for H_2O and D_2O. The MVIE of H_2O–D_2O is in the range of several tenths of a percent (see a review of Jancso et al., 1993). The EOS developed by Kestin et al. (1984a,b) can provide the molar volumes at a given pressure and temperature with high accuracy on the order of a few thousandths to a few hundredths of a percent (see a comparison between experimental data and those from the EOS in Table 1).

The applicability of this EOS-based approach (Eqs. (11)–(13)) for calculating the RIPFR for real gases can be tested by examining D_2O and H_2O fractionation between the liquid and vapor phases

$$H_2O_{\mathrm{liquid}}+D_2O_{\mathrm{vapor}}\leftrightarrow D_2O_{\mathrm{liquid}}+H_2O_{\mathrm{vapor}} \tag{14}$$

and

$$\begin{aligned}
&\ln\alpha_{\mathrm{L-V(D_2O)}}=\ln(s^*/s)f_{\mathrm{L}}-\ln(s^*/s)f_{\mathrm{V}}\\
&=\frac{A(T,\rho_{\mathrm{L}})-A(T,\rho_{\mathrm{V}})}{RT}-\frac{A^*(T,\rho_{\mathrm{L}})-A^*(T,\rho_{\mathrm{V}})}{RT},
\end{aligned} \tag{15}$$

where subscripts L and V denote the liquid and vapor phases, respectively. In order to compare the calculated

Table 1
A comparison of the MVIE in heavy (D_2O) and ordinary (H_2O) water estimated by Kell (1977) and that calculated from the EOS of Kestin et al. (1984a,b)

T (°C)	Molecular volume (cm^3/mol)				MVIE, $\frac{V_{D_2O}-V_{H_2O}}{V_{H_2O}} \times 10^3$	
	H_2O		D_2O			
	Kell (1977)	EOS	Kell (1977)	EOS	Kell (1977)	EOS
10	18.0206	18.0199	18.1080	18.1078	4.85	4.88
15	18.0314	18.0308	18.1099	18.1096	4.35	4.37
20	18.0476	18.0471	18.1185	18.1181	3.93	3.93
25	18.0685	18.0683	18.1331	18.1326	3.58	3.56
30	18.0939	18.0938	18.1531	18.1525	3.27	3.24
35	18.1233	18.1234	18.1779	18.1775	3.01	2.98
40	18.1565	18.1566	18.2072	18.2069	2.79	2.77
45	18.1932	18.1934	18.2406	18.2406	2.61	2.60
50	18.2333	18.2335	18.2779	18.2782	2.45	2.46
55	18.2766	18.2767	18.3190	18.3195	2.32	2.34
60	18.3230	18.3230	18.3634	18.3643	2.21	2.25
65	18.3724	18.3723	18.4113	18.4124	2.12	2.18
70	18.4247	18.4246	18.4623	18.4637	2.04	2.12
75	18.4799	18.4797	18.5165	18.5181	1.98	2.08
80	18.5380	18.5376	18.5737	18.5755	1.93	2.04
85	18.5988	18.5984	18.6338	18.6358	1.88	2.01
90	18.6624	18.6619	18.6968	18.6991	1.85	1.99
95	18.7287	18.7282	18.7628	18.7652	1.82	1.97
100	18.7978	18.8002	18.8316	18.8369	1.80	1.95

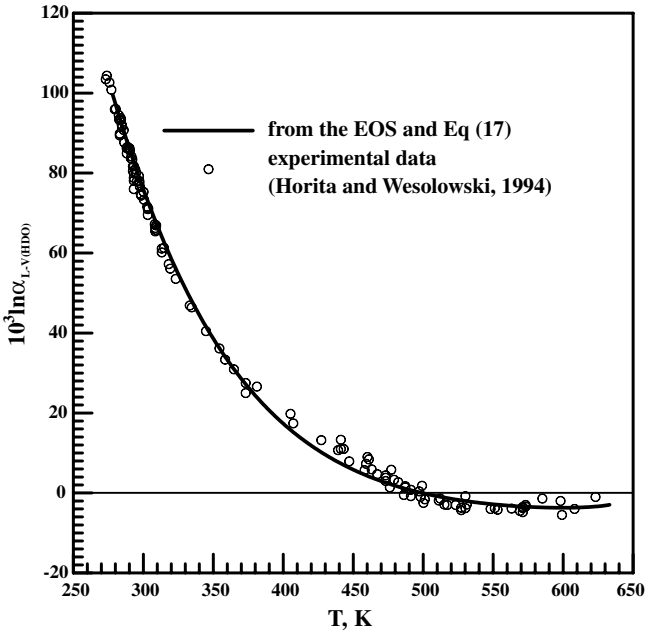

Fig. 3. Comparison of the liquid–vapor fractionation factor of HDO–H_2O calculated from the EOS (Method 2) with mass spectrometric measurements (Horita and Wesolowski, 1994).

values of $\ln \alpha_{L-V(D_2O)}$ with experimental values of $\ln \alpha_{L-V(HDO)}$ for the reaction

$$H_2O_{liquid} + HDO_{vapor} \leftrightarrow HDO_{liquid} + H_2O_{vapor} \quad (16)$$

the deviation from the rule of the geometric mean has to be taken into account (Polyakov et al., 2005)

$$\begin{aligned} &2\ln \alpha_{L-V(HDO)} - \ln \alpha_{L-V(D_2O)} \\ &\quad = (\rho_L - \rho_{cr})/T[(5.6938 \pm 0.1418)(1 - T/T_{cr}) \\ &\qquad - (18.7921 \pm 0.4156)(1 - T/T_{cr})^2 \\ &\qquad + (35.2445 \pm 0.4463)(1 - T/T_{cr})^3] \times 10^{-3}. \end{aligned} \quad (17)$$

Theoretical calculations of the value of $\ln \alpha_{L-V(HDO)}$ from Eqs. (15) and (17) agree very well with those obtained from direct mass spectrometric measurements by Horita and Wesolowski (1994) (Fig. 3).

Another example is hydrogen isotope fractionation between liquid water and gaseous hydrogen. Assuming hydrogen gas behaves ideally at temperatures above 273 K and at low pressures, a D/H fractionation factor between liquid water and gaseous hydrogen can be written as

$$\begin{aligned} \ln \alpha_{H_2O(l)-H_2} = &\ln(s^*/s)f_{ideal\text{-}HDO} - \ln(s^*/s)f_{ideal\text{-}H_2} \\ &+ \frac{1}{2}\left[\frac{A(T,\rho)-A(T,0)}{RT} - \frac{A^*(T,\rho)-A^*(T,0)}{RT}\right]_{water} \\ &+ \frac{1}{2}(\rho_L - \rho_{cr})/T[(5.6938 \pm 0.1418)(1 - T/T_{cr}) \\ &- (18.7921 \pm 0.4156)(1 - T/T_{cr})^2 \\ &+ (35.2445 \pm 0.4463)(1 - T/T_{cr})^3] \times 10^{-3}, \end{aligned} \quad (18)$$

where the term $\ln(s^*/s)f_{ideal\text{-}HDO} - \ln(s^*/s)f_{ideal\text{-}H_2}$ relates to hydrogen isotope fractionation between ideal water vapor and ideal hydrogen gas, and the term $\frac{1}{2}\left[\frac{A(T,\rho)-A(T,0)}{RT} - \frac{A^*(T,\rho)-A^*(T,0)}{RT}\right]_{water}$ describes the density effect on $\ln(s*/s)f_{HDO}$ according to the rule of the geometric mean. The remaining terms in Eq. (18) refer to the deviation from the rule of the geometric mean along the water liquid–vapor equilibrium curve (Polyakov et al., 2005).

Using the RIPFR of ideal-gas H_2 from Bardo and Wolfsberg (1975), an excellent agreement is achieved between calculations and experimental data of Rolston et al. (1976) (Fig. 4). These two examples demonstrate the validity of the EOS-based method for calculating the RIPFR for real fluids.

4. Reduced isotope partition function ratios of water at elevated pressures

Using Method 2 developed above, we can determine the pressure dependence of the RIPFR for real H_2O–D_2O fluids. The pressure effect can be expressed as the ratio of the RIPFR at a given pressure to that at a reference pressure (Horita et al., 2002)

$$\Gamma_P \equiv \frac{(s^*/s)f(T,P)}{(s^*/s)f(T,P_{ref})}. \quad (19)$$

A similar quantity Γ_ρ can be introduced for the density effect. Zero pressure (density) is chosen as reference state for the gas and supercritical fluid phases, whereas the saturated water vapor pressure along the liquid–vapor bound-

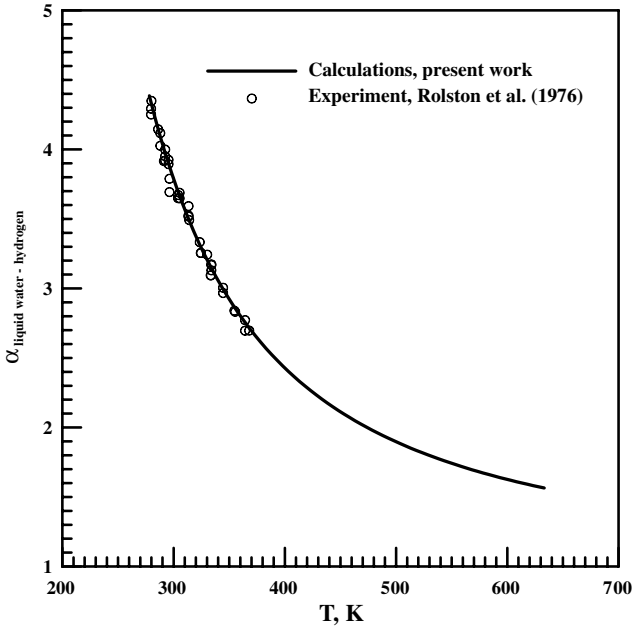

Fig. 4. Comparison of the hydrogen isotope fractionation factor for the system liquid water–H_2 calculated from the EOS (Method 2) and mass spectrometric measurements (Rolston et al., 1976).

ary is used as the reference for the liquid phase. Assuming that the pressure effect obeys the rule of the geometric mean, one can write following expressions.

Gas phase and super critical fluids:

$$\ln \Gamma_{\mathrm{P(HDO)}} \equiv \ln(s^*/s) f_{\mathrm{HDO}}(T,P) - \ln(s^*/s) f_{\mathrm{HDO}}(T,0) = \frac{G(T,P) - G(T,0)}{2RT} - \frac{G^*(T,P) - G^*(T,0)}{2RT} \quad (20)$$

or

$$\ln \Gamma_{\rho(\mathrm{HDO})} \equiv \ln(s^*/s) f_{\mathrm{HDO}}(T,\rho) - \ln(s^*/s) f_{\mathrm{HDO}}(T,0) = \frac{A(T,\rho) - A(T,0)}{2RT} - \frac{A^*(T,\rho) - A^*(T,0)}{2RT}. \quad (21)$$

Liquid phase:

$$\ln \Gamma_{\mathrm{P(HDO)}} \equiv \ln(s^*/s) f_{\mathrm{HDO}}(T,P) - \ln(s^*/s) f_{\mathrm{HDO}}(T,P_{\mathrm{sat}}) = \frac{G(T,P) - G(T,P_{\mathrm{sat}})}{2RT} - \frac{G^*(T,P) - G^*(T,P_{\mathrm{sat}})}{2RT} \quad (22)$$

or

$$\ln \Gamma_{\rho(\mathrm{HDO})} \equiv \ln(s^*/s) f_{\mathrm{HDO}}(T,\rho) - \ln(s^*/s) f_{\mathrm{HDO}}(T,\rho_{\mathrm{L}}) = \frac{A(T,\rho) - A(T,\rho_{\mathrm{L}})}{2RT} - \frac{A^*(T,\rho) - A^*(T,\rho_{\mathrm{L}})}{2RT}. \quad (23)$$

The factor 2 in the denominators of Eqs. (20)–(23) stems from the rule of the geometric mean between H_2O and D_2O.

Results of our calculations for the pressure (density) effect on the RIPFR for HDO–H_2O are shown in Figs. 5–7 for water vapor, liquid water, and supercritical water, respectively. For water vapor at temperatures from 10 to 336 ± 1 °C, the RIPFR of real HDO–H_2O fluids increases very slightly (up to +1.3 in the unit of $10^3 \ln \Gamma_{\mathrm{P}}$ and $10^3 \ln \Gamma_{\rho}$) with increasing pressure or density until the pressure reaches that of the liquid–vapor boundary (Fig. 5). However, at 350 °C the values of $10^3 \ln \Gamma_{\mathrm{P}}$ and $10^3 \ln \Gamma_{\rho}$ increase by +0.9 at 13 MPa (0.076–0.080 g/cm^3), then decrease slightly toward the liquid–vapor boundary. The pressure effect of liquid water is opposite in direction. From the saturated vapor pressure to 100 MPa, the values of $10^3 \ln \Gamma_{\mathrm{P}}$ and $10^3 \ln \Gamma_{\rho}$ always decrease by 0.5–2‰ (Fig. 6), and the magnitude of the pressure effect increases with increasing temperature from 30 to 350 °C. At the liquid–vapor boundary, there exists isotope fractionation (Fig. 3), whose magnitude is much greater than that attributable to pressure effects.

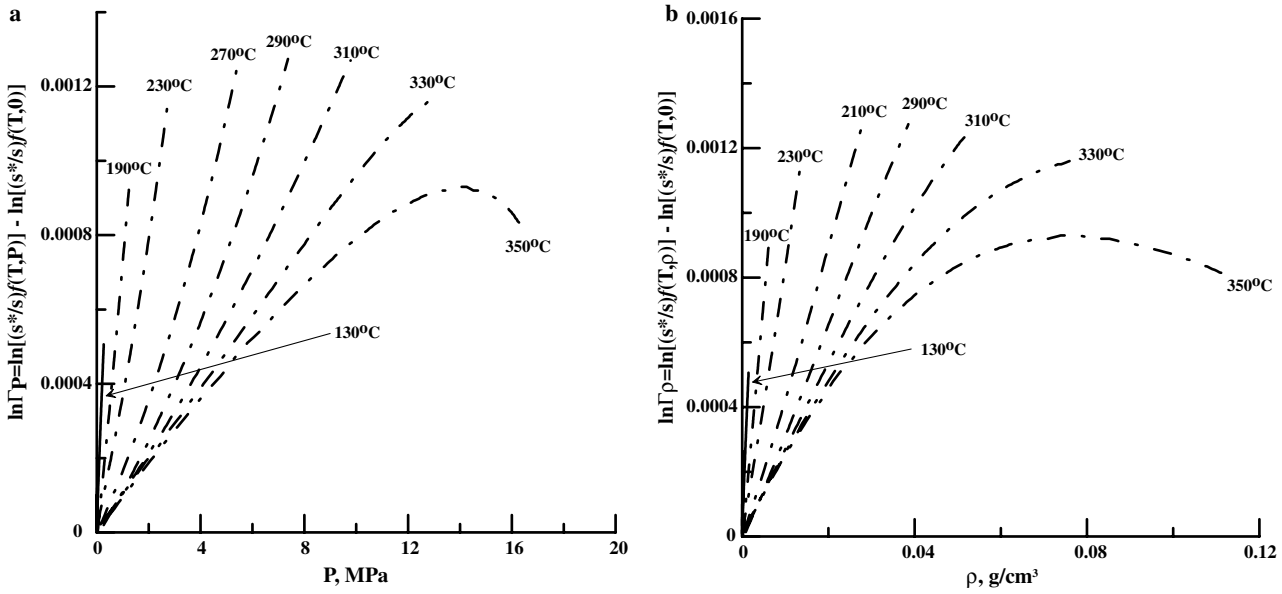

Fig. 5. (a) Pressure and (b) density effects on the RIPFR of water vapor calculated from the EOS (Method 2).

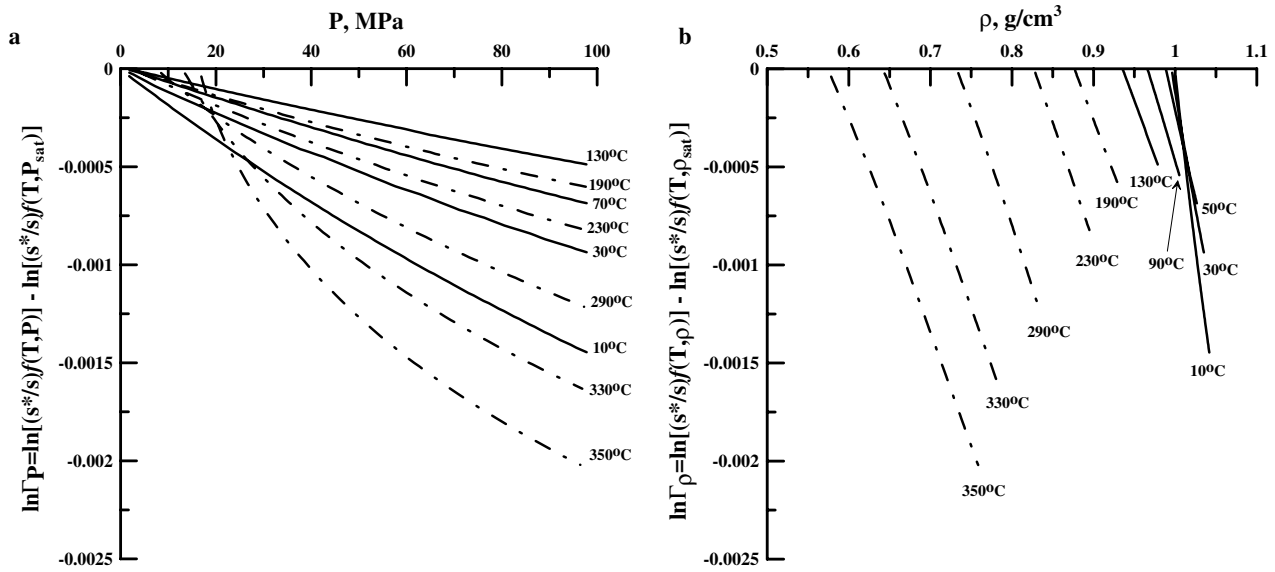

Fig. 6. (a) Pressure and (b) density effects on the RIPFR of liquid water relative to that at saturation vapor pressure, calculated from the EOS (Method 2).

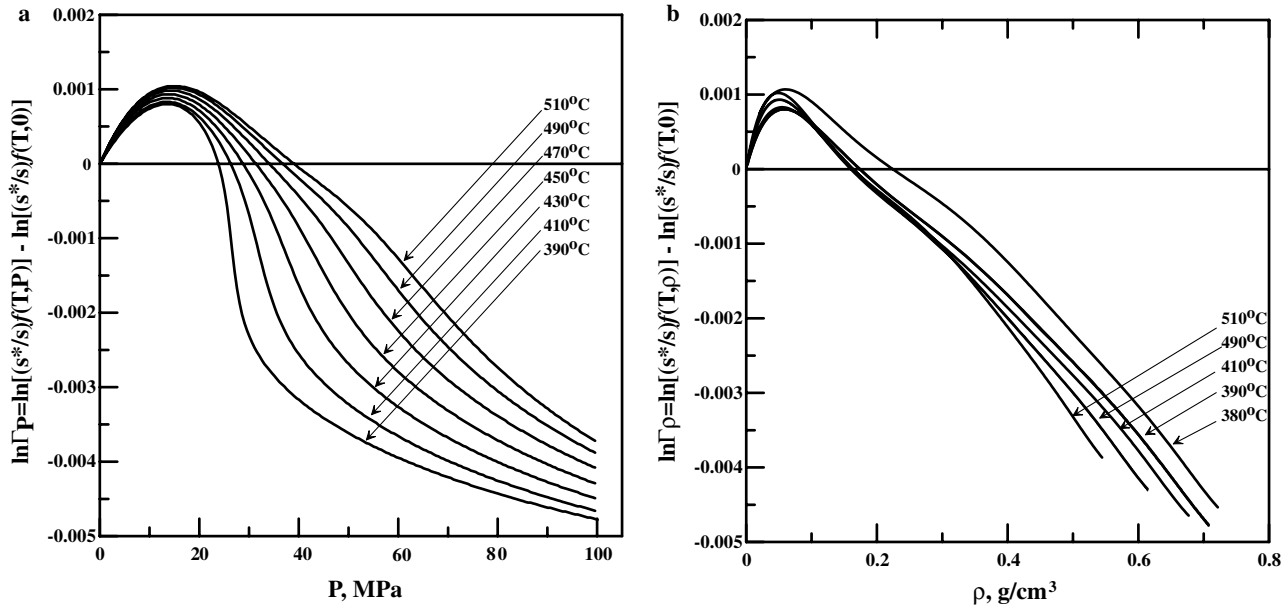

Fig. 7. (a) Pressure and (b) density effects on the RIPFR of supercritical water calculated from the EOS (Method 2).

In supercritical water, the values of $10^3 \ln \Gamma_P$ and $10^3 \ln \Gamma_\rho$ first increase slightly (ca. 1‰) with increasing pressure from 0 to 14 MPa, attain maximum values at 14 MPa (density of 0.04–0.06 g/cm^3), then decrease gradually by 5–6‰ with increasing pressure to 100 MPa (Fig. 7). The net pressure effects from 0 to 100 MPa range from −4 to −5‰. These results agree qualitatively with the previous theoretical estimations by Polyakov and Kharlashina (1994) and Driesner (1997). Considering the thermodynamic relationship $(\frac{\partial \ln(s^*/s)f}{\partial P})_T = -\frac{V^*-V}{RT}$ (Clayton et al., 1975), this complex behavior of the pressure effect on HDO–H_2O fluids can be readily explained by the fact that the water vapor and low-density supercritical water have a normal MVIE ($\Delta V = V^* - V < 0$), but the liquid water and high-density supercritical water have an inverse MVIE ($\Delta V = V^* - V > 0$). The maxima in Figs 5 and 7 correspond to P–T conditions where MVIE has a crossover (MVIE = 0). Horita et al. (2002) reported experimental results of the pressure effect on brucite–water hydrogen isotope fractionation at temperature from 200 to 600 °C and at pressure up to 800 MPa. Taking into account small positive pressure effects on the RIPFR of brucite (Horita et al., 2002), their experimental results agree well with our theoretical calculations of the pressure effects on water in this study (see Horita et al. (2002) for detailed discussion of pressure (density) effects on mineral-water fractionation). A good linear relation-

ship observed between the value of $10^3 \ln \Gamma_\rho$ and the density of water (Fig. 7b) suggests that water density could be used as a proxy for estimating the isotope pressure effects in water beyond the pressure limit of EOS for D_2O (100 MPa).

5. Conclusions

A simple, yet rigorous thermodynamic method was established for calculating the RIPFR of HDO–H_2O fluids at elevated temperatures (to 527 °C) and pressures (to 100 MPa), using the EOS of D_2O and H_2O from the literature. The validity of this approach was tested by comparing our results of EOS-based isotope fractionations of liquid–vapor water and liquid water–H_2 with experimental data in the literature. Successful application of this method to water or any other fluids depends on the accuracy of: (a) RIPFR of "ideal-gas" isotopic species and (b) the EOS of endmember isotopic species available from the literature. The former defines the RIPFR at infinitely low pressure (density) and the latter allows the calculations of the pressure (density) effect on the RIPFR relative to that of "ideal-gas," using the pressure dependency of the free energies of pure isotopic species.

Our calculations demonstrate that the RIPFR of HDO–H_2O exhibits a complex pressure dependence. For water vapor, the RIPFR increases slightly (ca. 0.5–1 in the value of $10^3 \ln \Gamma_P$ and $10^3 \ln \Gamma_\rho$) to the saturation vapor pressure at 10–336 °C. From 336 to 350 °C, the value of $10^3 \ln \Gamma_P$ increases first, then very slightly (0.2‰) decreases above 13 MPa to the saturation vapor pressures. In the liquid phase, the value of $10^3 \ln \Gamma_P$ always decrease by 0.5–2‰ with increasing pressure to 100 MPa. The value of $10^3 \ln \Gamma_P$ for supercritical water first increases slightly (1‰) to 15 MPa, then decreases by 4–5‰ to 100 MPa. Water is unique in that the pressure effect on the RIPFR is negative in liquid and high-density supercritical fluids, due to its inverse MVIE. This is the main cause for the experimental results of large (up to 12‰) increases in the hydrogen isotope fractionation factor between brucite, $Mg(OH)_2$, and water (Horita et al., 2002). In light of increasing recognition of the role of water and aqueous fluids in the subduction zone and the mantle, it is of great geochemical importance to understand the pressure effect on the isotopic properties of water and other fluids beyond the temperature and pressure ranges of this study.

Acknowledgments

We thank E. Shauble and two other reviewers for their valuable comments. Research was sponsored by the Division of Chemical Sciences, Geosciences, and Biosciences, Office of Basic Energy Sciences, U.S. Department of Energy, under contract DE-AC05-00OR22725, Oak Ridge National Laboratory, managed by UT-Battelle, LLC and by Scientific Program # 7 of Geoscience Department of Russian Academy of Sciences.

Associate editor: Thomas Chacko

References

Abdulkadirova, K.S., Wyczalkowska, A.K., Anisimov, M.A., Sengers, J.V., 2002. Thermodynamic properties of mixtures of H_2O and D_2O in the critical region. *J. Chem. Phys.* **116**, 4597–4610.

Bardo, R.D., Wolfsberg, M., 1975. A theoretical calculation of the equilibrium constant for the isotopic exchange reaction between H_2O and HD. *J. Phys.* **80**, 1068–1070.

Bardo, R.D., Wolfsberg, M., 1977. The wave equation of a non-linear triatomic molecule and the adiabatic correction to the Born-Oppenheimer approximation. *J. Chem. Phys.* **67**, 593–603.

Bardo, R.D., Wolfsberg, M., 1978. The adiabatic correction for nonlinear triatiomic molecules: techniques and calculations. *J. Chem. Phys.* **68**, 2686–2695.

Bigeleisen, J., 1961. Statistical mechanics of isotope effects on the thermodynamic properties of condensed systems. *J. Chem. Phys.* **34**, 1485–1493.

Bigeleisen, J., Mayer, M.G., 1947. Calculation of equilibrium constants for isotope exchange reactions. *J. Chem. Phys.* **15**, 261–267.

Bopp, P., Heinzinger, K., Vogel, P.C., 1974. Calculations of the oxygen isotope fractionation between hydration water of cations and free water. *Z. Naturforsch* **29a**, 1608–1613.

Bron, J., Chang, C.F., Wolfsberg, M., 1973. Isotopic partition function ratios involving H_2, H_2O, H_2S, HSe and NH_3 Z. *Naturforsch* **28a**, 129–136.

Chialvo, A.A., Horita, J., 2003. Isotopic effect on phase equilibria of atomic fluids and their mixtures: a direct comparison between molecular simulation and experiment. *J. Chem. Phys.* **119**, 4458–4467.

Clayton, R.N., Goldsmith, J.R., Karel, K.J., Mayeda, T.K., Newton, R.C., 1975. Limits on the effect of pressure on isotopic fractionation. *Geochim. Cosmochim. Acta* **39**, 1197–1201.

Driesner, T., 1997. The effect of pressure on deuterium-hydrogen fractionation in high temperature water. *Science* **277**, 791–794.

Driesner, T., Seward, T.M., 2000. Experimental and simulation study of salt effects and pressure/density effects on oxygen and hydrogen stable isotope liquid–vapor fractionation for 4 molal NaCl and KCl aqueous solutions to 400 °C. *Geochim. Cosmochim. Acta* **64**, 1773–1784.

Driesner, T., Ha, T.-K., Seward, T.M., 2000. Oxygen and hydrogen isotope fractionation by hydration complexes of Li^+, Na^+, K^+, Mg^{2+}, F^-, Cl^-, and Br^-: a theoretical study. *Geochim. Cosmochim. Acta* **64**, 3007–3033.

Harvey, A.H., Lemmon, E.W., 2002. Correlation for the vapor pressure of heavy water from the triple point to the critical point. *J. Phys. Chem. Ref. Data* **31**, 173–181.

Hill, P.G., 1990. A unified fundamental equation for the thermodynamic properties of H_2O. *J. Phys. Chem. Ref. Data* **19**, 1233–1274.

Hill, P.G., MacMillan, R.D.C., Lee, V., 1982. A fundamental equation of state for heavy water J. *Phys. Chem. Ref. Data* **11**, 1–14.

Horita, J., Wesolowski, D.J., 1994. Liquid–vapor fractionation of oxygen and hydrogen isotopes of water from the freezing to the critical temperature. *Geochim. Cosmochim. Acta* **58**, 3425–3437..

Horita, J., Cole, D.R., Polyakov, V.B., Driesner, T., 2002. Experimental and theoretical study of pressure effects on hydrogen isotope fractionation in the system brucite–water at elevated temperatures. *Geochim. Cosmochim. Acta* **66**, 3769–3788.

Jàkli, VanHook, W.A., 1981. D/H and $^{18}O/^{16}O$ fractionation factors between vapor and liquid water. *Geochem. J.* **15**, 47–50.

Jancso, G., Rebelo, L., Van Hook, W.A., 1993. Isotope effects in solution thermodynamics: excess properties in solutions of isotopomers. *Chem. Rev.* **93**, 2645–2966.

Jancso, G., Van Hook, W.A., 1974. Condensed phase isotope effects (especially vapor pressure isotope effects). *Chem. Rev.* **74**, 589–750.

Jones, W.M., 1968. Vapor pressures of tritium oxide and deuterium oxide. Interpretation of the isotope effects. *J. Chem. Phys.* **48**, 207–213.

Kell, G.S., 1977. Effect of isotopic composition, temperature, pressure, and dissolved gases on the density of liquid water. *J. Phys. Chem. Ref. Data* **6**, 1109–1131.

Kestin, J., Sengers, J.V., Kamgar-Parsi, B., Levelt Sengers, J.M.H., 1984a. Thermophysical properties of fluid H_2O. *J. Phys. Chem. Ref. Data.* **13**, 175–183.

Kestin, J., Sengers, J.V., Kamgar-Parsi, B., Levelt Sengers, J.M.H., 1984b. Thermophysical properties of fluid D_2O. *J. Phys. Chem. Ref. Data.* **13**, 601–609.

Kiselev, S.B., 1997. Prediction of the thermodynamic properties and the phase behavior of binary mixtures in the extended critical region. *Fluid Phase Equilibria* **128**, 1–28.

Kondepudi, D., Prigogine, I., 1998. *Modern thermodynamics: from heat engines to dissipative structures*. Wiley, New York.

Kostrowicka-Wyczalkowska, A., Abdulkadirova, Kh.S., Anisimov, M.A., Sengers, J.V., 2000. Thermodynamic properties of H_2O and D_2O in the critical region. *J. Chem. Phys.* **113**, 4985–5002.

Kleinman, L.I., Wolfsberg, M., 1973. Correction to the Born-Oppenheimer approximation and electronic effects on isotopic exchange equilibria I. *J. Chem. Phys.* **59**, 2043–2051.

Landau L.D., Lifshits, E.M., 1980. Course of theoretical physics. Vol. 5. Statistical Physics. Part 1. Pergamon Press.

Liu, C.T., Lindsay Jr., W.T., 1970. Vapor pressure of deuterated water from 106 to 300 °C. *Chem. Eng. Data* **15**, 510–513.

Miles, F.T., Menzies, A.W.C., 1936. The vapor pressure of deuterium water from 20 to 230 °C. *J. Am. Chem. Soc.* **58**, 1067–1069.

Oliver, G.D., Grisard, J.W., 1956. Vapor pressure and critical constants of D_2O. *J. Am. Chem. Soc.* **78**, 561–563.

Polyakov, V.B., Kharlashina, N.N., 1994. Effect of pressure on equilibrium isotopic fractionation. *Geochim. Cosmochim. Acta* **58**, 4739–4750.

Polyakov, V.B., Horita, J., Cole, D.R., 2005. Isotopic self-exchange reactions of water: evaluation of the rule of the geometric mean in liquid–vapor isotope partitioning. *J. Phys. Chem. A* **109**, 8642–8645.

Richet, P., Bottinga, Y., Javoy, M., 1977. A review of hydrogen, carbon, nitrogen, oxygen, sulphur and chlorine stable isotope fractionation among gaseous molecules. *Ann. Rev. Earth Planet. Sci.* **5**, 65–110.

Riesenfeld, E.H., Chang, T.L., 1936. Dumpdruck und verdampfungswärme von schwerem wasser. *Z. Phys. Chem.* **B33**, 120–126.

Rolston, J.H., den Hartog, J., Butler, J.P., 1976. The deuterium isotope separation factor between hydrogen and liquid water. *J. Phys. Chem.* **80**, 1064–1067.

Singh, R.K., Wolfsberg, M., 1975. The calculation of isotopic partition functions ratio by perturbation theory technique. *J. Chem. Phys.* **62**, 4165–4180.

Urey, H.C., 1947. The thermodynamic properties of isotopic substances. *J. Chem. Soc. (Lond.)*, 562–581.

Wagner, W., Pruss, A., 2002. The IAPWS formulation1995 for the thermodynamic properties of ordinary water substance for general and scientific use. *J. Phys. Chem. Ref. Data* **31**, 387–535.

Williams, Q., Hemley, R.J., 2001. Hydrogen in the deep Earth. *Ann. Rev. Earth Planet Sci.* **29**, 365–418.

Zieborak, K., 1966. Siedetemperaturen und dampfdrücke von H_2O–D_2O–gemischen und deren azeotropen. *Z. Phys. Chem.* **231**, 248–258.